Plasmonics (2017) 12:977–986
DOI 10.1007/s11468-016-0349-4

Study of Surface Plasmon Resonances of Core-Shell Nanosphere: A Comparison between Numerical and Analytical Approach

Richa Sharma[1] · Sangita Roopak[1,2] · Nilesh kumar Pathak[1] · Alok ji[1] · R P Sharma[1]

Received: 12 May 2016 / Accepted: 1 August 2016 / Published online: 20 August 2016

Abstract An investigation of the wavelength dependent extinction spectra of coated sphere with different core@shell compositions based on discrete dipole approximation technique has been presented in this paper. We have used combinations of Ag, Au, and SiO_2 for this analysis. Specifically, we study the impact of *spherical* core-shell thickness on its surface plasmon resonance (SPR) *peak positions* and corresponding *spectral widening* in distinct regimes of the spectrum. We observe that SPR peak of core-shell nanoparticle(*CSNP*) can be tuned over the visible to near-infrared spectrum region by manipulating the core/shell ratio and composition of core and shell. Specifically, for dielectric@metal (core@shell) nanoparticle, SPR peak position shifted towards *lower* wavelength as we *increase* the shell thickness, which is opposite to the SPR behavior of metal@dielectric. The extinction spectrum shows *linear* relation between SPR position and thickness of the shell. Further, we observed two resonant peaks for the case of metal@metal CSNP. The SPR peak of Au@Ag (a_{eff} 100 nm with shell thickness 8 nm) reveals two resonant peak corresponding to Au (594 nm) in red domain, while the peak in blue domain corresponds to Ag (402 nm). We also observe that optical resonance of CSNP can be tuned across the near-infrared region by changing the surrounding medium of higher refractive index. Further, near field pattern of core@shell geometry at resonance wavelength is also shown in the present study. We have also compared the numerical and analyticalmethod for smaller size CSNP with varying thickness and the results show good agreement.

Keywords Plasmonics · Core-shell nanoparticle · Surface plasmon resonance · Dipole model · Discrete dipole approximation

Introduction

Metal nanoparticles (MNPs) demonstrate unusual optical properties in comparison to bulk materials. Smaller particle size gives rise to an increased surface area to volume ratio, which leads to an increase in the domination of the surface atoms over those in its interior [1, 2]. Nanoparticles (NPs) fall in numerous classes due to their different ways of fabrication, applications, and properties. Typically, noble metals such as Au (gold), Ag (silver), and Pt (platinum), etc. are used to make NPs. Au and Ag NP are useful in many applications like bio-tech and solar energy conversion because of their plasmonic properties. One of the extremely impressive optical properties of MNP is surface Plasmon resonance (SPR). It is related to charge density oscillation at the metallodielectric interface. These collective charge oscillations cause an extensive enhancement of the local electric field inside and close to the NP. SPR depends upon the size, shape, and surrounding environment of metal nanogeometry [3].

✉ Richa Sharma
richas330@gmail.com

[1] Centre for Energy Studies, Indian Institute of Technology, Delhi, India

[2] Physics Department, Mahila Vidyalaya Degree College, Ganga Prasad Road, Aminabad, Lucknow 226018, India

A very important class of MNP is core-shell nanoparticles (CSNPs) [4–6]. It draws attention due to its fascinating properties and wide range of applications such as catalysis [7, 8], creating photonic crystals [9], controlled drug release [10, 11], electronics [12], biomedical [13], pharmaceutical [14], photovoltaic and optics [14], etc. In CSNPs, inner material is defined as core and the outer coated material as shell. In comparison to non-coated nanosphere, two layer (core/shell) spherical nanoparticles provide an extra degree of freedom in SPR that can be tuned in the desired range of electromagnetic spectrum [15–17]. The advantage of the coated nanoparticle over non-coated nanoparticle is many fold, for example, stability, surface modification, reduction in consumption of precious material, and reduction in reactivity [18].

The SPR frequency of the hybrid particles will change according to the morphology of chosen NPs. Core and shell materials can be either organic or inorganic which depends on the end use applications [19–21]. There are several combinations of core@shell such as metal@dielectric, dielectric@metal and metal@metal geometries are widely used to study the SPRs. Utilization of these plasmonic resonances in various field of science, for example, optical transparency, colloidal stability, bio-compatibility, and easy surface modification [22]. To prevent the aggregation and deformation of Au and Ag, NPs silica coating is necessary and these metal coated dielectric materials are used for biomedical application [23]. Since Au is a material with powerful absorbing and scattering plasmonic properties, vast application of Au nanoshells such as biomedical field, for tumor cell imaging, drug delivery and many others [24]. The SPR peak of NP coated with Au material can be tuned from visible to near-infrared spectrum region only by adjusting the core/shell parameters [25, 26]. For chemical stability purpose Au is used as shell material which prevents the core material from oxidation and corrosion [27, 28]. The Au@Ag (core@Shell) systems have their own significance due to the wide tunability in its SPR peak position [29, 30]. Among Au- and Ag-based core@shell NPs, the use of Au@Ag CSNPs would be more beneficial than Ag@Au CSNPs because the Ag component have stronger optical property which is used as outer layer in Au@Ag [31].

Several models have been established to see the impact of optical properties, such as absorption, scattering, and extinction of CSNPs. There are two kinds of methodologies widely used to analyze the optical properties, one is analytical and other is numerical. Classical Mie scattering theory [32], finite difference time domain method (FDTD) [33], discrete dipole approximation (DDA) [34] has been verified to describe the optical response of core-shell nano-structures precisely. These formalisms require critical input parameter such as dielectric function of the metal nanostructures and embedding media.

The present manuscript gives the researchers a thought that they can take diverse materials for coated geometry to see its impacts on SPR peak positions and corresponding spectral widening in distinct regimes of the spectrum. In this paper, we are considering the spherical shape of CSNP with three different types of combinations in which one is noble metal (Ag and Au) used as a core and shell is made up of dielectric material ($Si\,O_2$), second one is dielectric material ($Si\,O_2$) used as a core and shell is made up of metal (Ag and Au) and the last combination is metal@metal (Ag@Au, Au@Ag). We demonstrate that by altering effective radii of NP and thickness of the shell there is wide tunability in SPR. To study the optical properties of above said nanogeometries, we have pursued analytical approach (dipole model) to discuss SPR and also compared the analytical results with numerical results. It is seen, dipole model is applicable only for smaller particle ($<$ 50 nm). Hence, for particle size greater than 50nm, one of the best suited numerical techniques DDA is used. In DDA, we used 268,096 polarizable dipoles to represent CSNP, which interact with the external field and among themselves. The optical properties of the NP are given by the summation of optical properties of all the constituent dipoles. Ubuntu 14.04(64-bit) running on Intel Xeon 3.10 GHz processor work station with RAM 132GB computing equipment is used for calculation.

Figure 1 shows the schematic diagram showing the effect of coating. SPR peak of non-coated silver nanosphere of effective radius 40 nm observed at 389 nm. When the silver nanosphere coated by $Si\,O_2$, the SPR peak gets red shifted to 413nm. The plasmon resonant frequency depends upon the refractive index of chosen nanogeometry. As the geometry changes corresponding effective refractive index changes that modify the plasmon resonant frequency which occurs only when the Frohlich condition is satisfied.

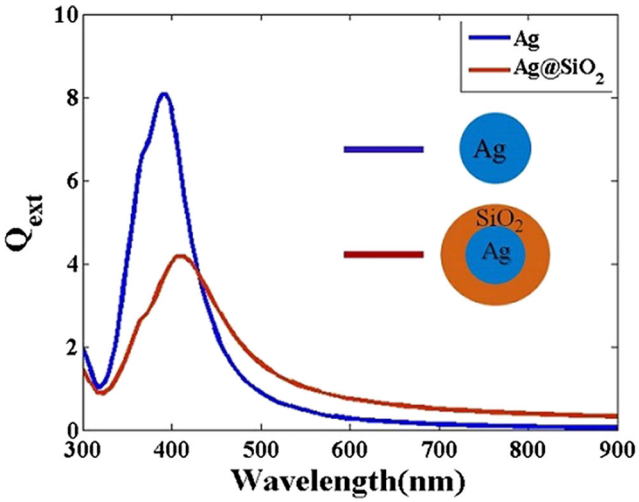

Fig. 1 Schematic of the extinction spectra of silver nanosphere and silver sphere coated with $Si\,O_2$

Methodology

To calculate the absorption and scattering efficiency of MNP, Dipole model (analytical approach) and DDA (Numerical approach) are utilized in the present manuscript. Dipole model is applicable for particle size much smaller than the wavelength of the incident light. For larger particle size, where the quasi-static approximation does not hold well due to phase change of applied field over the particle size, numerical approach is needed. Numerical techniques are based on surface and volume discretization and are more demanding than analytical method. DDA is one of the best numerical methods and well suited technique for studying scattering and absorption of electromagnetic radiations by a particle, with size of the order or less than that of the wavelength of the incident light.

Dipole Model

Dipole model is also known as quasi-static approximation. Quasi-static means phase of harmonically oscillating electromagnetic field is practically constant over the particle volume. Hence, particle feels harmonic oscillating field as electrostatic field. In this model, electric field outside the NP can be calculated by solving the Laplace equation with suitable boundary conditions. The field induced by the core@shell nanogeometry can be computed by the effective polarizability and dipole moment of the composite system as

$$p = \epsilon_m \alpha_{eff} E_0 \tag{1}$$

$$\alpha_{\text{eff}} = 4\pi b^3 \frac{(\epsilon_2\epsilon_a - \epsilon_m\epsilon_b)}{(\epsilon_2\epsilon_a + \epsilon_m\epsilon_b)} \tag{2}$$

For core@shell geometry, dielectric function is in ratio of the shell volume to the core volume

$$\epsilon_a = \epsilon_1(3 - 2f) + 2\epsilon_2 f \tag{3}$$

$$\epsilon_b = \epsilon_1 f + 2\epsilon_2(3 - f) \tag{4}$$

$$f = 1 - (\frac{a}{b})^3 \tag{5}$$

Where ϵ_1 and ϵ_2 represent the dielectric constant of the core and the shell respectively. Dielectric constant of embedding medium is represented by ϵ_m and f represents the ratio of the shell volume to the total volume of CSNP. Inner radius is represented by a and b is the outer radius of the core@shell system. Incident electric field is E_0, p is the effective dipole moment of the core@shell NP and α_{eff} represents the effective dipolar polarizability. The polarizability expression of core-shell nanoparticle related to the dielectric function as given in equation 2. When the denominator term $(\epsilon_2\epsilon_a + \epsilon_m\epsilon_b)$ of the polarizability expression is minimum, polarizability experienced a resonant enhancement.

Scattering and absorption enhancement of metallic nanostructure are main consequences of resonantly enhanced polarization. Hence, scattering and absorption cross section C_{sca} and C_{abs}, respectively, of metallic nanoparticle calculated via following relations.

$$C_{\text{sca}} = \frac{k^4}{6\pi}|\alpha_{\text{eff}}|^2 \tag{6}$$

$$C_{\text{abs}} = kIm[\alpha_{\text{eff}}] \tag{7}$$

By normalizing these scattering and absorption, cross section by total area of the core@shell nanogeometry gives rise to scattering and absorption efficiency Q_{sca} and Q_{abs}, respectively.

$$Q_{\text{sca}} = \frac{C_{\text{sca}}}{\pi b^2} \tag{8}$$

$$Q_{\text{abs}} = \frac{C_{\text{abs}}}{\pi b^2} \tag{9}$$

$$Q_{\text{ext}} = Q_{\text{sca}} + Q_{\text{abs}} \tag{10}$$

Discrete Dipole Approximation

Calculation of the extinction spectra is directed by the open source programming DDSCAT 7.1.0 [35], which calculate the absorption and scattering of target geometry by "discrete dipole approximation" [36]. DDA is a highly efficient and flexible method to study the extinction and absorption efficiencies of arbitrary size and shape of MNP which has been described in detail elsewhere [36]. The DDA starts by dividing the object into a cubic of N-point dipoles, located on a cubic lattice with lattice spacing d then the actual volume of solid material in the target is defined as $V = Nd^3$. The size of the target is characterized by effective radius (a_{eff}) which is the radius of an equal volume sphere and given by $a_{\text{eff}} = (\frac{3V}{4\pi})^{\frac{1}{3}}$.

Purcell and Pennypacker [37] used the Clausius-Mossotti polarizabilities to relate the dielectric function with the i^{th} element having polarizability.

$$\alpha_i = \frac{(\epsilon_s(r_i,\omega) - \epsilon_m(r_i,\omega))}{(\epsilon_s(r_i,\omega) + 2\epsilon_m(r_i,\omega))}\frac{3d^3}{4\pi} \tag{11}$$

$\epsilon_m(r_i,\omega)$ and $\epsilon_s(r_i,\omega)$ are medium and scattering dielectric function respectively. The scattering cross section can be calculated by

$$C_{\text{sca}} = C_{\text{ext}} - C_{\text{abs}} \tag{12}$$

With the extinction cross section

$$C_{\text{ext}} = \frac{4\pi k}{|E_{\text{inc}}|^2}\sum_{j=1}^{N} Im(E^*_{\text{inc}}.P_j) \tag{13}$$

and the absorption cross section

$$C_{\text{abs}} = \frac{4\pi k}{|E_{\text{inc}}|^2} \sum_{j=1}^{N} Im[P_j.\alpha_j^{-1} P_j^* - \frac{2}{3}k^3|P_j|^2) \quad (14)$$

Where E_{inc} is the incident electric field and k is the wave number, P is the polarization induced by each dipole, and * represent the complex conjugate. Dielectric constant of various material is a key requirement for calculation of optical properties of CSNP. Drude-Lorentz model gives the size dependent dielectric function of the MNP as

$$\epsilon(\omega) = \epsilon_{\text{bulk}}(\omega) + \frac{\omega_p^2}{\omega^2 + j\gamma_{\text{bulk}}\omega} - \frac{\omega_p^2}{\omega^2 + j(\gamma_{\text{bulk}} + A\frac{v_f}{R})\omega} \quad (15)$$

$\epsilon_{\text{bulk}}(\omega)$ is bulk metal dielectric constant, ω_p is the plasma frequency (1.36×10^{16} Hz for Ag and 1.37×10^{16} Hz for Au) and ω is the angular frequency of the incident field, γ_{bulk} is the electron collision damping in the metal, v_f is the Fermi velocity of electron, (1.39×10^6 m/s for Ag and 1.38×10^6 m/s for Au), A is the geometrical parameter and its value lies between 1 and 2, here A = 1.

Results and Discussions

Optical properties of CSNP depend on the size, shell thickness, and material composition of core and shell. Dipole model is valid for particle size less than 50 nm but it is no more valid for the larger size particle as charge distribution is no more homogeneous for large particle. Hence, there is a strong need of introducing another method to calculate optical properties of lager size nanoparticle (> 50 nm). Figure 2 represents the extinction specrta of $Ag@SiO_2$ CSNP of 10 nm effective radius with varying shell thickness (2 to 8 nm). The results obtained from Dipole model and DDA shows good agreement for 10 nm effective radius (a_{eff}). For example, using dipole model, SPR peak of $Ag@SiO_2$ of effective radius 10 nm (shell thickness −2 nm) is around 373 nm, whereas with DDA this peak is around 372 nm. Figures 2a, b plotted by using Eqs. 10 and 13, respectively. Since, for the larger particle size dipole model is not valid, we are using a numerical approach for further calculations (for larger size particle). The numerical algorithm really converges towards the dipole model as the number of dipoles grows which is clearly seen in Fig. 3a and b. However, this increment in number of dipoles results in higher computation complexity. Therefore, considering the current computational capabilities of a typical scientific workstation, we have limited N (number of dipoles) to be less than 10^6 for our numerical experiment.

Figure 4 represents the wavelength dependent extinction spectrum of CSNP ($Ag@SiO_2$) of three different effective radii 60, 80, and 100 nm embedded in air. Figure 4 shows that SPR peak amplitude goes down and also slightly red shifted as we increase the shell thickness. It is clearly seen from Fig. 4a, for 60 nm outer radius with shell thickness 2 nm, SPR peak position around 432 nm while for shell thickness 8 nm SPR peak position is at 453 nm. Further, for the case of 80 nm the extinction peak of $Ag@SiO_2$ CSNP with shell thickness 2 nm is around 493 nm which is shifted towards red domain (523 nm) of the electromagnetic spectrum for 8 nm shell thickness as shown in Fig. 4b. Similarly, Fig. 4c shows the similar trend of red shifting with increase in the shell thickness. So we conclude that the extinction peak shows red shift with increase in the shell thickness although highest extinction peak amplitude obtained for minimum shell thickness.

Figure 4 shows the calculated spectra of the efficiency of extinction (Qext) for CSNP $Au@SiO_2$ embedded in air using the same CSNP parameters as we have used for the study of $Ag@SiO_2$. $Au@SiO_2$ SPR peak followed similar trend of the red shifting with increase in the shell thickness as for the case of $Ag@SiO_2$. Here, we observe higher λ_{max} (at which maximum resonance occur) for $Au@SiO_2$ in comparison to that of $Ag@SiO_2$. For example, taking 100 nm effective radius with shell thickness 2 nm of $Au@SiO_2$, we have found SPR peak position around 614 nm while for the case of $Ag@SiO_2$ SPR peak position was around 593 nm.

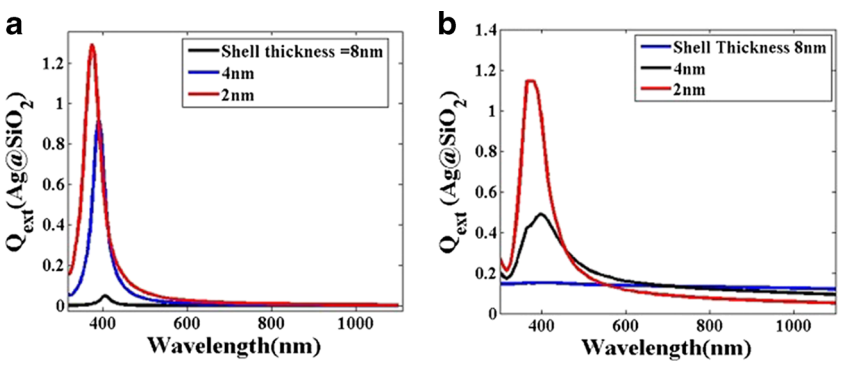

Fig. 2 Q_{ext} as a function of wavelength of $Ag@SiO_2$ CSNP of effective radius 20 nm with shell thickness 2 nm embedded in air **a** DDA for discretization of dipoles (33,552 to 268,096). **b** Dipole model

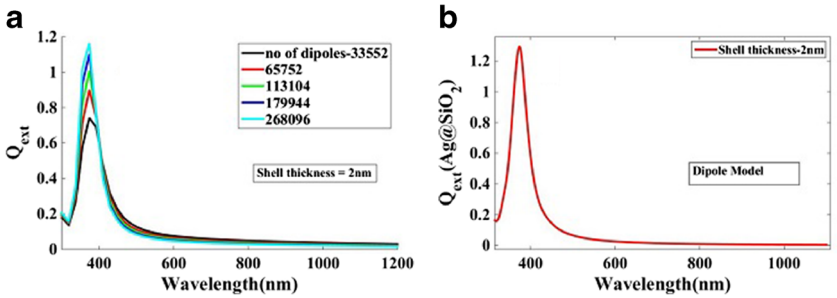

Fig. 3 Extinction Spectra of $Ag@SiO_2$ CSNP of radius 10 nm using **a** Dipole model **b** DDA method

Figure 6 shows the extinction spectra of $SiO_2@Ag$ with a_{eff} 60, 80, and 100 nm embedded in air in which dielectric material chosen as a core and metal as a shell. It is observed from the Fig. 6, for dielectric@metal ($SiO_2@Ag$) CSNP SPR peak position shifted towards lower wavelength as we increase the shell thickness which is opposite to the SPR behavior of metal@dielectric CSNP (Figs. 4 and 5). The extinction peak appeared at 665 nm for 60 nm radius of $SiO_2@Ag$ with shell thickness 2 nm and it is shifted towards the blue domain (593 nm) of the electromagnetic spectrum for shell thickness 8 nm. For minimum shell thickness, we observed the maximum red shifting along with the broadening of the spectrum. Dielectric function has real and imaginary part, in which real part contribute to the polarization and imaginary part related with the energy dissipation which is zero for dielectric material. In case of dielectric@metal, on increasing the shell thickness (metal ratio increases in CSNP or dielectric material ratio decreases), energy dissipation becomes more which shifts the SPR peak towards lower wavelength. Figure 7 represents the extinction spectra of $SiO_2@Au$ CSNP with a_{eff} 60, 80, and 100 nm embedded in air for different shell thickness. The results are consistent in terms of shell thickness and spectral shift as discussed for the case of $SiO_2@Ag$. Here also, we have observed blue shifting of the SPR peak with increase in the shell thickness.

Now we discuss the optical behavior of metal@metal CSNP with varying shell thickness for effective radius 60, 80, and 100 nm embedded in air as shown in Fig. 8 (Ag@Au) and Fig. 9 (Au@Ag). Here, we observed different behavior of extinction spectra of Ag@Au (Fig. 8) and Au@Ag (Fig. 9) in terms of spectral shift with shell thickness. For the case of Ag@Au, SPR peak position is blue shifted with the decreased shell thickness. On the other hand, for the case of Au@Ag, SPR peak position shows red shift with the decreased shell thickness. The reason of blue shifting on decreasing the shell thickness for the case of Ag@Au is due to the reduction of Au content on

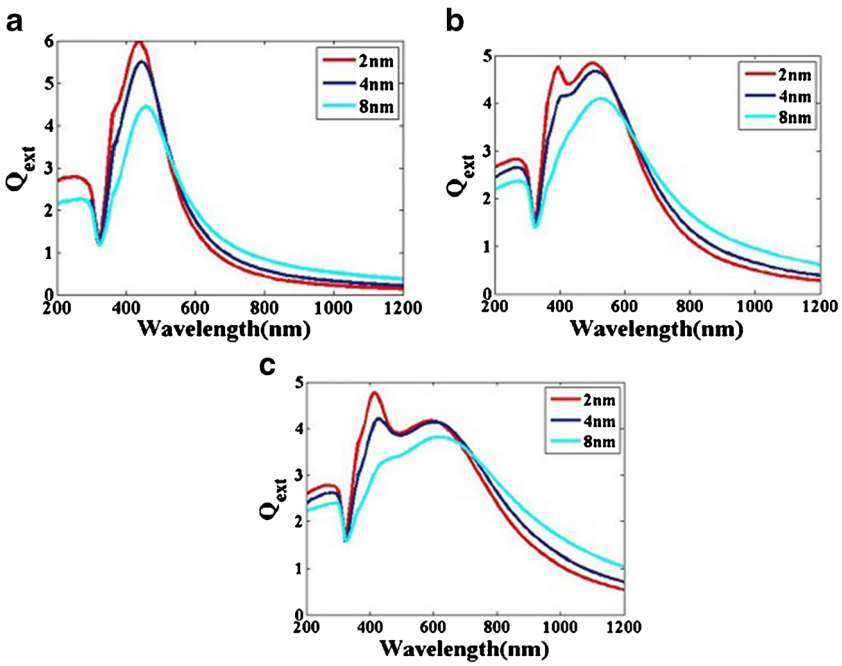

Fig. 4 Extinction spectra of core@shell(Ag@SiO_2) nanosphere embedded in air with three different shell thickness (2 to 8 nm) with effective radius set to **a** 60 nm, **b** 80 nm, and **c** 100 nm

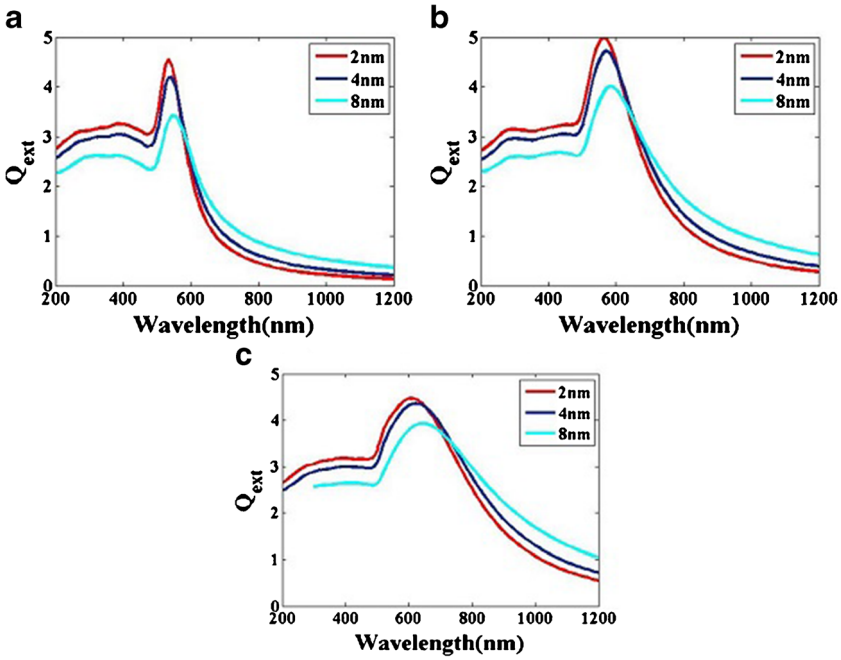

Fig. 5 Extinction spectra of $Au@SiO_2$ CSNP embedded in air with three different shell thickness with effective radius **a** 60, **b** 80, and **c** 100 nm

reducing the shell thickness. The inter-band transitions are more important in case of Au as compare to Ag. Further, we have found two resonant peaks for the case of metal@metal (Au@Ag and Ag@Au) CSNP. Out of these two cases of metal@metal CSNP, we have selected Au@Ag to discuss the SPR peak positions. For the case of Au@Ag CSNP SPR peak at higher wavelength corresponds to Au, and an additional peak at shorter wavelength of electromagnetic spectrum corresponds to Ag. SPR peak corresponds to Au core is at 533 nm for a_{eff} 80 nm with Ag shell thickness 8 nm, which is shifted towards red domain (543 nm) on decreasing the thickness of Ag shell about 2 nm. On the other hand, SPR peak corresponds to Ag shell is at 361 nm for a_{eff} 80 nm with shell thickness 8 nm, which is shifted towards the blue domain (351 nm) of the electromagnetic spectrum on decreasing the shell thickness (4 nm).

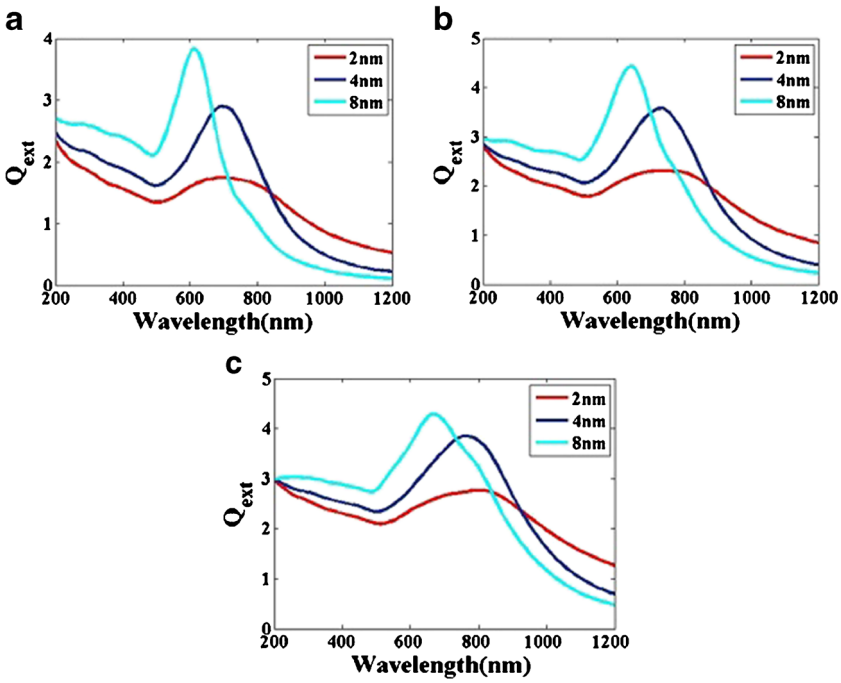

Fig. 6 Extinction spectra of SiO_2 NP coated with Ag ($SiO_2@Ag$) with three (2, 4, and 8 nm) shell thickness with effective radius **a** 60, **b** 80, and **c** 100 nm

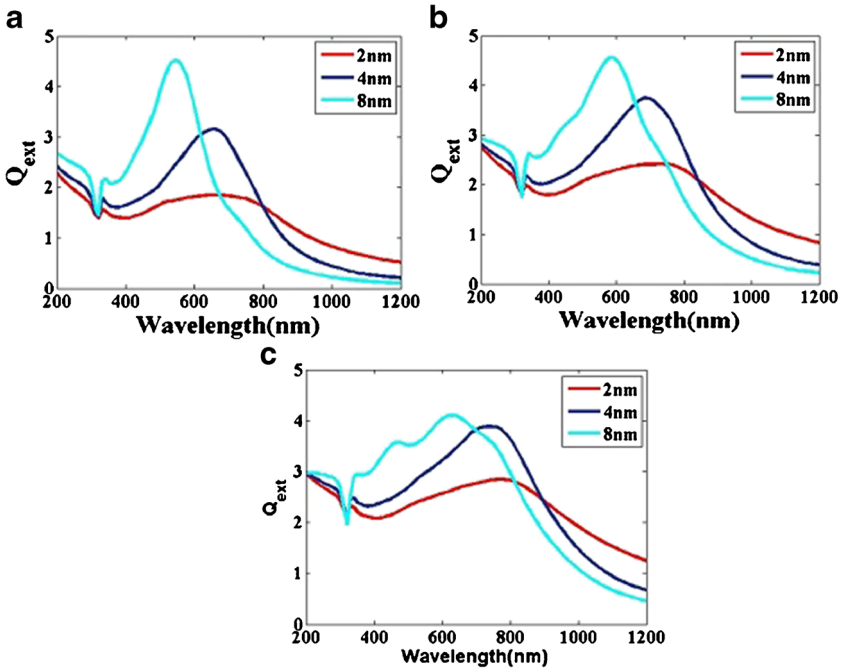

Fig. 7 Extinction spectra of $Si\,O_2@Au$ sourrounded with air with different Shell thickness with a_{eff} set to **a** 60 nm, **b** 80 nm, and **c** 100 nm

Surrounding medium has a great impact on the optical behavior of CSNP. The polarizability expression of core-shell nanoparticle related to the dielectric function is given in Eq. 2. When the denominator term $(\epsilon_2\epsilon_a + \epsilon_m\epsilon_b)$ of the polarizability expression is minimum, polarizability experienced a resonant enhancement To see the influence of surrounding medium, extinction spectra have been plotted for $Si\,O_2@Ag$ of radius 20 nm embedded in different environment air and Si. It was observed that as we increase the refractive index of the surrounding medium SPR peak position shifted towards higher wavelength followed by broadening of the spectrum. When the surrounding medium (silicon) gets polarized, restoring force for the core decreases and the resonance peak gets shifted towards higher wavelength. It is seen that the SPR peak amplitude of the $Si\,O_2@Ag$ embedded in Si is higher as compare to those of embedded in air. For instance, in case of air, the SPR peak position is observed at 401 nm with amplitude 3 (Fig. 10a) while it is shifted toward IR region (964 nm with amplitude 12) for silicon (Fig. 10b) for the case of a_{eff} 20 nm with shell

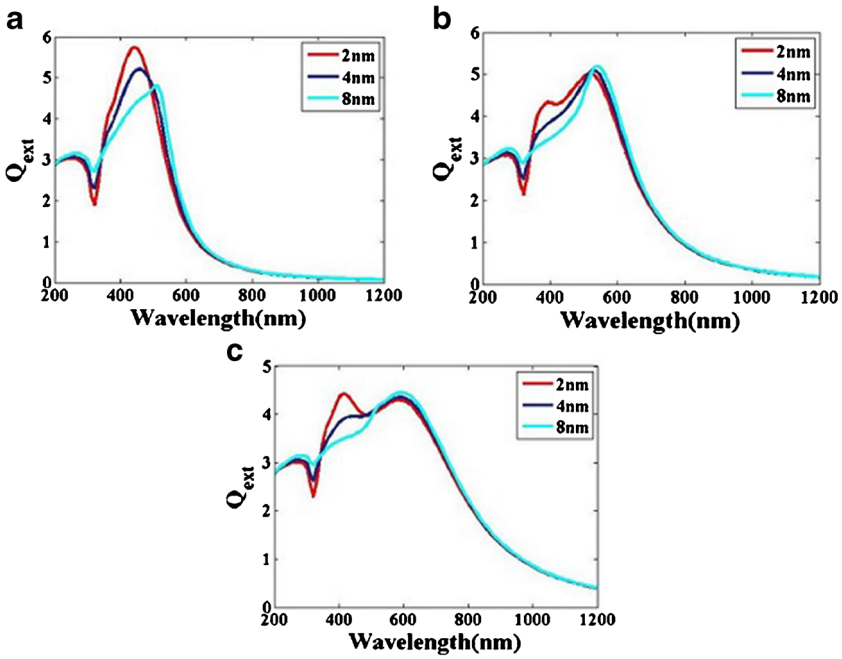

Fig. 8 Extinction spectra of metal@metal (Ag@Au) nanosphere embedded in air with different shell thickness (2 to 8 nm) with a_{eff} **a** 60 nm, **b** 80 nm, and **c** 100 nm

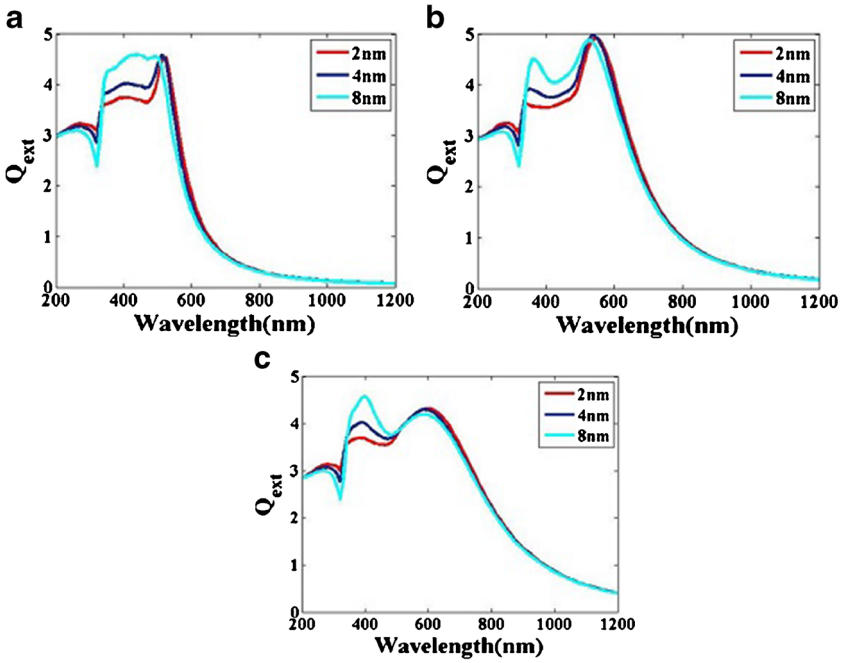

Fig. 9 Extinction spectra of Au@Ag nanosphere embedded in air with different shell thickness (2nm to 8 nm) with a_{eff} **a** 60 nm, **b** 80 nm, and **c** 100 nm

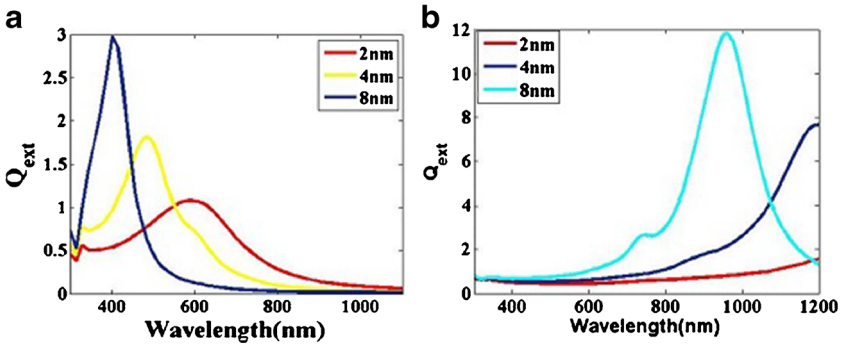

Fig. 10 Extinction spectra of $SiO_2@Ag$ embedded in **a** air and **b** Si with different Shell thickness (2 to 8 nm) with a_{eff} 20 nm

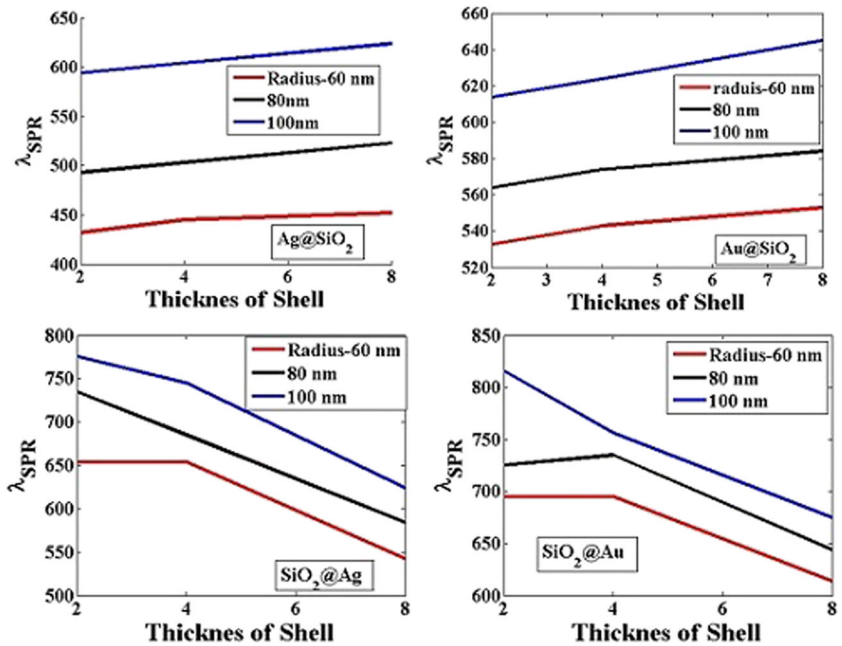

Fig. 11 Variation of peak value of resonant wavelength (λ_{SPR}) with shell thickness

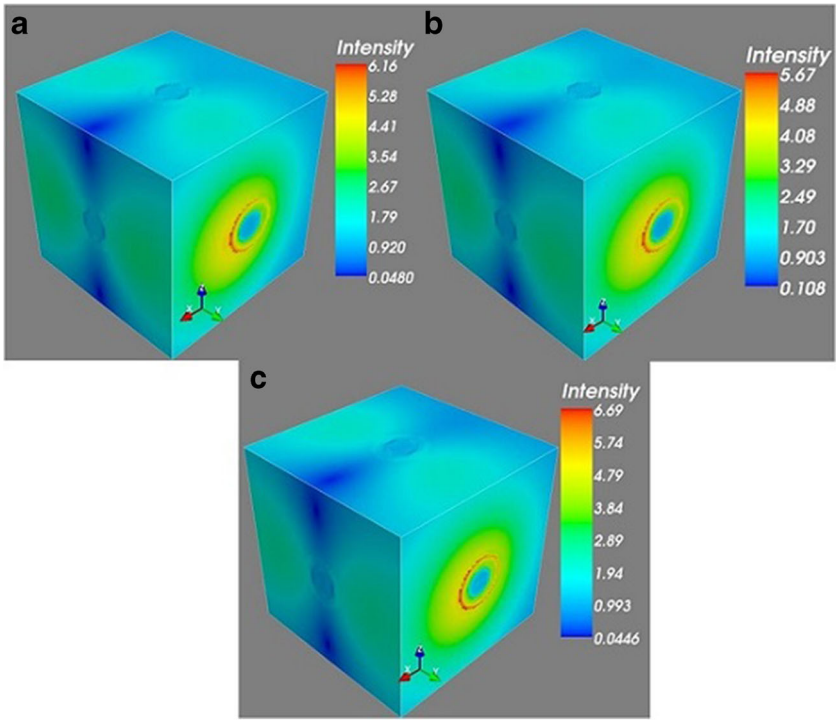

Fig. 12 Near field pattern of CSNP Ag@Au of effective radius 60 nm with the thickness of the shell **a** 2 nm, **b** 4 nm, and **c** 8 nm. The excitation wavelengths are **a** 442 nm, **b** 452 nm, and **c** 513 nm

thickness 8 nm. Similar to $SiO_2@Ag$ in air, we observed increased extinction efficiency along with the blue shifting on increasing the shell thickness for $SiO_2@Ag$ in Si.

Figure 11 gives the correlation between thickness of the shell and SPR peak position. In case of metal@dielectric CSNP, we observe the red shift with the increased shell thickness. On the other hand, dielectric@metal CSNP SPR peak position is blue shifted with the increased shell thickness.

Figure 12 represents the three-dimensional field distribution of core@shell at resonance wavelength. Increased enhancements are found near the surface of the NP as the thickness of the Au shell increased. It is noticed that there are few spots close to the shell surface that have high enhancement of near field. This field enhancement gives rise to enormous optical cross-sections for molecules in the vicinity.

Conclusions

We simulated CSNP with various combinations (metal@dielectric, dielectric@metal, and metal@metal) to study the tunability of SPR peak. We have found that SPR depends upon the thickness of shell, size of CSNP, surrounding environment, and the material chosen for core and shell. The present study gives an idea about the useful combinations of core@shell materials for various application purposes. Extinction peak for metal@dielectric case shows *red shift* with *increase* in the shell thickness although highest magnitude of extinction peak was obtained for minimum shell thickness. On the other hand, dielectric@metal CSNP SPR peak position shifts towards lower wavelength as we increase the shell thickness which is opposite to the SPR behaviour of metal@dielectric. For the case of Ag@Au core@shell NP, we observed that decreasing the shell thickness leads to the blue shifting of the electromagnetic spectrum. On the other hand, for Au@Ag core/shell NP, decreasing the shell thickness leads to *red shift* and broadening of the spectrum. It was observed that as we increase the refractive index of the surrounding medium, SPR peak broadens and its position shifts towards *higher* wavelength of electromagnetic spectrum. We have also observed increased near field enhancement for Ag@Au core shell geometry with increase in the thickness of Au shell.

References

1. Wang FX, Rodríguez FJ, Albers WM, Ahorinta R, Sipe JE, Kauranen M (2009) Phys Rev B 80:233402
2. Atwater HA, Polman A (2009) Nat Mater 9:205
3. Noguez C (2007) J Phys Chem C 111:3806
4. Wang F, Deng R, Wang J, Wang Q, Han Y, Zhu H, Chen X, Liu X (2011) Nat Mater 10:968
5. Zhang J, Misra R (2007) Acta Biomaterialia 3(6):838
6. Caruso F (2001) Adv Mater 13:11
7. Wang AQ, Chang CM, Mou CY (2005) J Phys Chem B 109(40):18860

8. Wei X, Yang XF, Wang AQ, Li L, Liu XY, Zhang T, Mou CY, Li J (2012) J Phys Chem C 116(10):6222
9. Scodeller P, Flexer V, Szamocki R, Calvo EJ, Tognalli N, Troiani H, Fainstein A (2008) J Am Chem Soc 130(38): 12690
10. Sounderya N, Zhang Y (2008) Recent Patents on Biomedical Engineering (Discontinued), vol 1
11. Yan E, Ding Y, Chen C, Li R, Hu Y, Jiang X (2009) Chem Commun:2718–2720
12. Lauhon LJ, Gudiksen MS, Wang D, Lieber CM (2007) Nature 420:57
13. Balakrishnan S, Bonder MJ, Hadjipanayis GC (2009) J Magn Magn Mater 321(2):117
14. Yang Z, Niu Z, Lu Y, Hu Z, Han CC (2003) Angew Chem Int Ed 42:1943
15. Prodan E, Nordlander P (2003) Nano Lett 3(4):543
16. Pathak NK, Pandey GK, Ji A, Sharma R (2015) Plasmonics 10(6):1597
17. Pathak NK, Ji A, Sharma R (2014) Plasmonics 9(3):651
18. Kalele S, Gosavi SW, Urban J, Kulkarni SK (2006) Curr Sci 91(8):1038
19. Park HH, Woo K, Ahn JP (2013) Sci Rep:3
20. Jiang HL, Akita T, Ishida T, Haruta M, Xu Q (2011) J Am Chem Soc 133(5):1304. doi:10.1021/ja1099006
21. Douvalis AP, Zboril R, Bourlinos AB, Tucek J, Spyridi S, Bakas T (2012) J Nanopart Res 14(9):1
22. Liu F, Rao BS, Nunzi JM (2011) Org Electron 12(7):1279
23. Vanderkooy A, Chen Y, Gonzaga F, Brook MA (2011) ACS Appl Mater Interfaces 3(10):3942
24. Hirsch LR, Stafford RJ, Bankson JA, Sershen SR, Rivera B, Price RE, Hazle JD, Halas NJ, West JL (2003) Proc Natl Acad Sci 100(23):13549
25. Yang P, Yan H, Mao S, Russoand R, Johnson J, Saykally R, Morris N, Pham J, He R, Choi HJ (2002) Adv Funct Mater 12(5):1616
26. Loo C, Lowery A, Halas N, West J, Drezek R (2005) Nano Lett 5(4):709
27. Lingyan Wang LW, Luo J, Fan Q, Suzuki M, Suzuki IS, Engelhard MH, Lin Y, Kim N, Wang JQ, Zhong CJ (2005) J Phys Chem B 109(46):21593
28. Zanella R, Sandoval A, Santiago P, Basiuk VA, Saniger JM (2006) J Phys Chem B 110(17):8559
29. Monga A, Pal B (2015) New J Chem 39:304
30. Lim DK, Kim IJ, Nam JM (2008) Chem Commun:5312–5314
31. Pande S, Ghosh SK, Praharaj S, Panigrahi S, Basu S, Jana S, Pal A, Tsukuda T, Pal T (2007) J Phys Chem C 111(29):10806
32. Bohren CF, Huffman DR (2007) Absorption and Scattering by a Sphere (Wiley-VCH Verlag GmbH)
33. Yang Z, Aizpurua J, Xu H (2009) J Raman Spectrosc 40(10):1343
34. Flatau PJ, Draine BT (2012) Opt Express 20(2):1247
35. Draine BT, Flatau PJ (2012) ArXiv e-prints
36. Draine BT, Flatau PJ (1994) J Opt Soc Am A 11(4):1491
37. Purcell EM, Pennypacker CR (1973) Astrophysical 186:705